Organic Electronics 13 (2012) 464–468

Contents lists available at SciVerse ScienceDirect

Organic Electronics

journal homepage: www.elsevier.com/locate/orgel

Letter

Spin cast self-assembled monolayer field effect transistors

Daniel O. Hutchins [a], Orb Acton [a], Tobias Weidner [b], Nathan Cernetic [a], Joe E. Baio [b], Guy Ting [c], David G. Castner [b], Hong Ma [a], Alex K.-Y. Jen [a,c,*]

[a] Department of Materials Science and Engineering, University of Washington, Seattle, WA 98195, United States
[b] Department of Bioengineering, University of Washington, Seattle, WA 98195, United States
[c] Department of Chemistry, University of Washington, Seattle, WA 98195, United States

ARTICLE INFO

Article history:
Received 14 August 2011
Received in revised form 24 October 2011
Accepted 23 November 2011
Available online 24 December 2011

Keywords:
Self assembled monolayer field effect transistor (SAMFET)
Organic field effect transistor (OFET)
Spin cast

ABSTRACT

Top-contact self-assembled monolayer field-effect transistors (SAMFETs) were fabricated through both spin-coating and solution assembly of a semiconducting phosphonic acid-based molecule (11-(5‴-butyl-[2,2′;5′,2″;5″,2‴;5‴,2⁗]quinquethiophen-5-yl)undecylphosphonic acid) (BQT-PA). The field-effect mobilities of both spin-cast and solution assembled SAMFETs were 1.1–8.0 × 10^{-6} cm^2 V^{-1} s^{-1} for a wide range of channel lengths (between 12 and 80 μm). The molecular monolayers were characterized by atomic force microscopy (AFM), attenuated total reflectance-Fourier transform infrared spectroscopy (ATR-FTIR), and near edge X-ray absorption fine structure (NEXAFS) spectroscopy. It was found that the BQT-PA monolayer films exhibit dense surface coverage, bidentate binding, and tilt angles of ~32° and ~44° for the thiophene rings and alkyl chain, respectively. These results indicate that rapid throughput of fabricating SAMFETs is possible even by spin-coating.

1. Introduction

In recent years, organic field effect transistors (OFETs) have become the subject of intense research due to the appeal of inexpensive, solution processed, and mechanically flexible electronic devices [1]. Possible applications include radio frequency identification tags, smart card, and drivers for active matrix displays [2]. Solution processing of organic molecules allows for the construction of various layers of device architecture by high-throughput and inexpensive means. Frequently studied is the use of π-conjugated organic molecules to form semiconducting films/layers [3].

The development of π-conjugated self-assembled monolayer (SAM) molecules has resulted in a new type of OFET; the self-assembled monolayer field effect transistor (SAMFET). Functionally, SAMFETs are OFETs in which the organic semiconductor is a single layer of well-packed π-conjugated molecules capable of acting as a charge-transporting channel. Fabrication of SAMFET devices has been attempted by several groups, however, most devices required channel lengths of submicrometer to ensure a gate voltage dependence of the source to drain channel current apparently due to limited lateral interconnection of the semiconducting SAM [4–7]. Recently, SAMFETs with long channel lengths up to 40 μm have been demonstrated by Smits et al., in which a SAM was formed on a silica gate dielectric via a greater than 15 h immersion phase assembly [8]. Performance of these SAMFETs was comparable to that of OFETs constructed with a three-dimensional bulk film.

In this paper, we demonstrate rapidly processed SAMFETs achieved through spin-coating a phosphonic acid-based molecule 11-(5‴-butyl-[2,2′;5′,2″;5″,2‴;5‴,2⁗]quinquethiophen-5-yl)undecylphosphonic acid (BQT-PA). The resulting spin-cast SAMs show uniform density, and well-ordered monolayer coverage comparable to that observed by conventional immersion phase solution assembly. The top-contact SAMFETs processed by spin-coating and immersion assembly show identical electronic performance.

* Corresponding author at: Department of Materials Science and Engineering, University of Washington, Seattle, WA 98195, United States.
E-mail address: ajen@u.washington.edu (A.K.-Y. Jen).

1566-1199/$ - see front matter © 2011 Elsevier B.V. All rights reserved.
doi:10.1016/j.orgel.2011.11.025

2. Materials and methods

2.1. BQT-PA synthesis

BQT-PA was synthesized by Pd-catalyzed coupling between diethyl 11-(5′-bromo[2,2′]bithiophen-5-yl)undecylphosphonate and (5″-butyl[2,2′;5′,2″]terthiophen-5-yl)trimethyltin at 90 °C in toluene to afford diethyl BQT-phosphonate. By reacting with bromotrimethylsilane, the diethyl BQT-phosphonate was converted into ditrimethylsilyl BQT-phosphonate and then hydrolyzed to afford the target molecule BQT-PA.

2.2. SAMFET device fabrication

The architecture of the SAMFET device studied in this work is presented in Fig. 1. Heavily *p*-doped silicon substrates with a 300 nm thermal oxide layer were used as a gate and dielectric material. A thin (~2 nm) aluminum oxide (Al_2O_3) adhesion layer was formed via a plasma-enhanced deposition to promote the binding of the phosphonic acid headgroups. BQT-PA was assembled on the Al_2O_3 adhesion layer by either spin-coating at 3000 rpm from a 2 mM chloroform solution followed by a 10-min of annealing at 140 °C or by 16 h immersion assembly in a 0.1 mM chlorobenzene solution. After either spin-coating or immersion assembly, SAM covered substrates were immersed in chlorobenzene held at 100 °C for 10 min, followed by spin rinsing with chlorobenzene to get rid of unbound molecules. All SAM processing occurred in a dry N_2 environment, followed by the thermal deposition of 50 nm thick gold to form source and drain electrodes to complete the top-contact SAMFETs. There is no indication that either the evaporation of gold or our cleaning procedure substantially damaged the SAM, as device performance of bulk BQT-PA films are comparable to that of the monolayer. In addition, the BQT-PA molecule was strategically designed with the butyl-terminal group to provide protection of the semiconducting core from the penetration of gold during thermal evaporation.

3. Results and discussion

As it has been demonstrated that charge transport in OFETs primarily occurs in the first few nanometers of the channel closest to the dielectric material, devices utilizing a single molecular layer for charge transport are attainable [9]. This ultra-thin semiconductor architecture has been shown to be highly desirable from the standpoint of chemical sensing, as slight electrochemical changes in the active layer result in measurable shifts in device performance [10]. One such method of obtaining a single molecular semiconducting layer is through formation of a π-conjugated self-assembled monolayer. Understanding the electronic/morphological properties of these SAMs as a function of molecular design is critical to achieving reproducible SAMFET-based sensing devices. Also important in this pursuit, is the development of processing methods that allow for increased speed of densely packed monolayer formation.

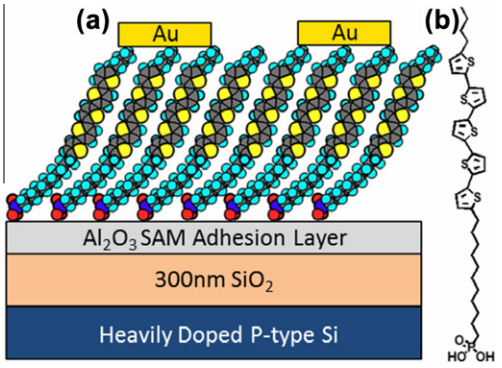

Fig. 1. (a) SAMFET device architecture (cartoon). From bottom: *p*-doped Si with 300 nm oxide, 2 nm adhesion layer, BQT-PA, gold electrodes. (b) Chemical structure of BQT-PA.

3.1. Spectral characterization of SAM (ATR-FTIR)

The morphology of SAMs formed from both spin-coated and solution assembled samples was characterized by atomic force microscopy (AFM). The images obtained show that the active SAM layers are comprised of a single monolayer with minimal surface aggregate (Fig. 2c). Characterization of the SAM by attenuated total reflectance-Fourier transform infrared spectroscopy (ATR-FTIR) was used to examine the binding mode of the molecule. Data in the ν_{PO} region show the presence of $\nu_{P=O}$ stretching at 1230 cm^{-1} as well as skeletal vibrations of phosphonate at 1110 cm^{-1} (Fig. 2a). Due to the lack of well resolved ν_{P-O-H} vibrations at 900–1000 cm^{-1}, we infer that the phosphonate binding is predominantly bidentate [11,12].

3.2. Spectral characterization of SAM (NEXAFS)

Near edge X-ray absorption fine structure (NEXAFS) spectroscopy can provide chemical identification of specific bonds within SAMs and detailed information about molecular alignment. Fig. 2b shows C K-edge spectra of BQT-PA SAMs collected at an X-ray incidence angle of 55°. At an incident angle of 55°, the spectra are independent of orientation effects (the so-called magic angle of NEXAFS). Within both spectra are characteristic absorption resonances at ~287.7 eV (R^*/C—H σ^*), and ~293.3 eV (C—C σ^*) related to the aliphatic carbon chains and a feature at ~285.6 eV (C—C π^*) related to the thiophene rings [13,14,16,17]. In addition, no features related to contamination were present (i.e. a C=O related resonance near 288.5 eV) [13,14]. NEXAFS angle dependencies for both spin-coated and immersion-assembled, can be found in Fig. 2b. Both SAMs exhibit positive and negative dichroism for the R^* and σ^* resonances, respectively, indicating that the SAMs are oriented upright [15]. Molecular orbitals related to the R^* transition are oriented perpendicular to the alkyl chain axis while those related to transitions into the C—C and C—C′ σ^* orbitals are orthogonally oriented parallel to the chain axis. The π^* resonances exhibit pronounced positive dichroisms indicating the rings are orientated upright.

For a more quantitative analysis of these angle dependencies, the tilt angles with respect to the surface normal of the *n*-alkyl chains and the ring structures were determined from the dichroisms at the R^* and π^* resonances,

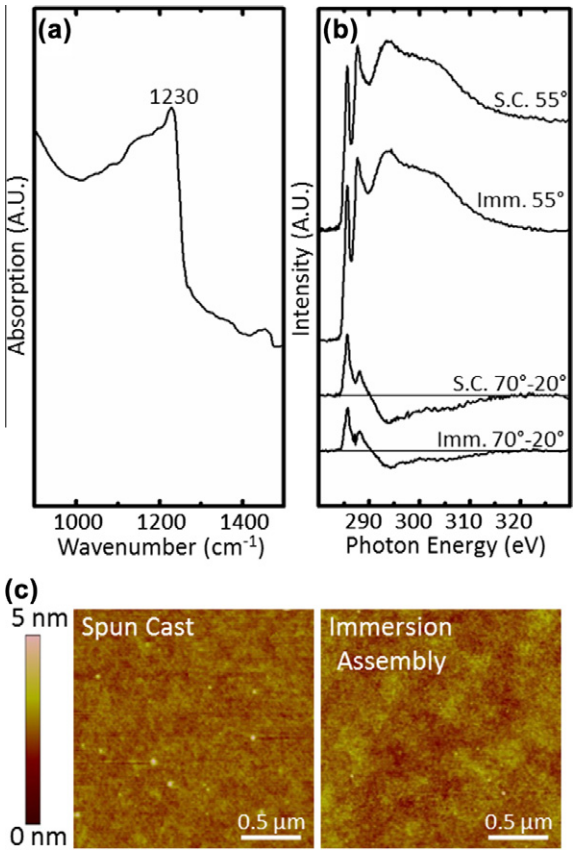

Fig. 2. (a) ATR-FTIR spectra showing bidentate binding modes for BQT-PA. (b) NEXAFS data of both 55° and 70–20° spectra for spin-cast (SC) and immersion assembly (Imm) SAMs. (c) AFM image of spin-cast (left) and immersion assembled (right) SAM surface.

respectively. The intensities of these resonances as a function of the X-ray incidence angle are evaluated for the spectra taken at 70°, 55° and 20° using published procedures for vector orbitals [13,16]. From this data the average tilt angles for both spin-coated and immersion assembled SAMs were found to be 43.3 ± 5.0° and 44.0 ± 5.0° for the alkyl chain (R*/C—H σ* orbital) and 30.4 ± 5.0° and 34.2 ± 5.0° for the thiophene rings (C—C π* orbital), respectively.

3.3. SAMFET device performance

Transistor characterization was performed in a N_2 environment using an Agilent 4155B semiconductor parameter analyzer. Top-contact SAMFET devices fabricated from the BQT-PA molecule demonstrated typical OFET output and transfer characteristics despite the active layer being comprised of only a single monolayer (Fig. 3). The output and transfer curves were found to be consistent for both immersion-assembled and spin-coated devices, as both exhibited similar electronic properties (Fig. 3a and b). The field effect mobility (μ) was calculated in the saturation regime using a linear fit of $(-I_{ds})^{1/2}$ vs. V_{gs}. The threshold voltage (V_t) was estimated as the x-intercept of the linear section of the plot of $(-I_{ds})^{1/2}$ vs. V_{gs}. Reported electrical characteristics are from more than 10 devices from a batch and averaged over two different batches (Table 1). These devices were found to have an average μ of 1.1–8.0 × 10^{-6} cm^2 V^{-1} s^{-1} for a wide range of channel lengths (device channel lengths measured were 12, 20, 30, 50 and 80 μm). On/off current ratio (I_{on}/I_{off}) for most devices was on the order of 10^2.

Since spin coating is inherently a batch process, an attempt at using a concentrated (2 mM BQT-PA in chlorobenzene) solution to achieve comparable SAMFET performance via rapid immersion assembly was carried out in order to examine the feasibility of reel to reel processing. Devices were fabricated after immersion in solution for 1 min, 5 min, 10 min, 30 min, 1 h and 5 h, followed by cleaning via the method outlined in Section 2.2. Ten transistors (all 12 μm channel length) were tested for each immersion period; their performance can be found in Table 2. It was shown that for less than 10 min immersion time, there was no gate voltage dependent current flow. With 10 min of immersion assembly, device performance was rarely existent except for a few functional SAMETs; of those that worked, mobility was on the order of ~10^{-8} cm^2 V^{-1} s^{-1}. With 30 min immersion, several SAMFET devices started to exhibit comparable performance to spun cast devices; however, most of these SAMFETs failed to exhibit the characteristic μ of ~10^{-6} cm^2 V^{-1} s^{-1}. With 1 h assembly, SAMFET performance was comparable to that of spun cast or 16 h dilute solution assembly devices. Although this 1 h immersion assembly time frame could potentially facilitate a continuous fabrication process that may offer greater throughput than the spin coating–annealing processing detailed, it is difficult to quantify at what scale of production this becomes advantageous. However, for laboratory and small batch settings, spin coating is still a less time intensive process.

Charge carrier mobility of our BQT-PA SAMFETs is comparable to those of SAMFETs based on quarter thiophene phosphonic acid molecules, yet inferior to the device performance from monofunctional chlorosilane SAMFETs with the same π-conjugated segment [7,8]. We believe this could be attributed to inherently different material/chemical properties of the phosphonic acid molecule and the aforementioned silane. First, it has been demonstrated that frequently used alkyl-phosphonic acid SAM molecules which are commonly regarded as highly ordered and densely packed, exhibit an inherent tilt angle of ⩾30° much like BQT-PA [18]. The intrinsic tilt angle of the phosphonic acid could result in decreased wave function overlap and inferior charge transport properties relative to the monofunctional chlorosilane molecule which is tilted at 10°. Second, the silane based chemistry used by Smits et al., as stated in their supporting information, forms not a true monolayer that may have resulted in increased device performance [7]. Unbound molecules and π-conjugated synthetic byproducts could have adsorbed to the bound monolayer increasing packing density/forming a multilayer, thereby improving the electronic properties of the SAM. It was also stated by the authors that if this phenomenon occurred, it could not be determined with the spectroscopic methods employed in the characterization of

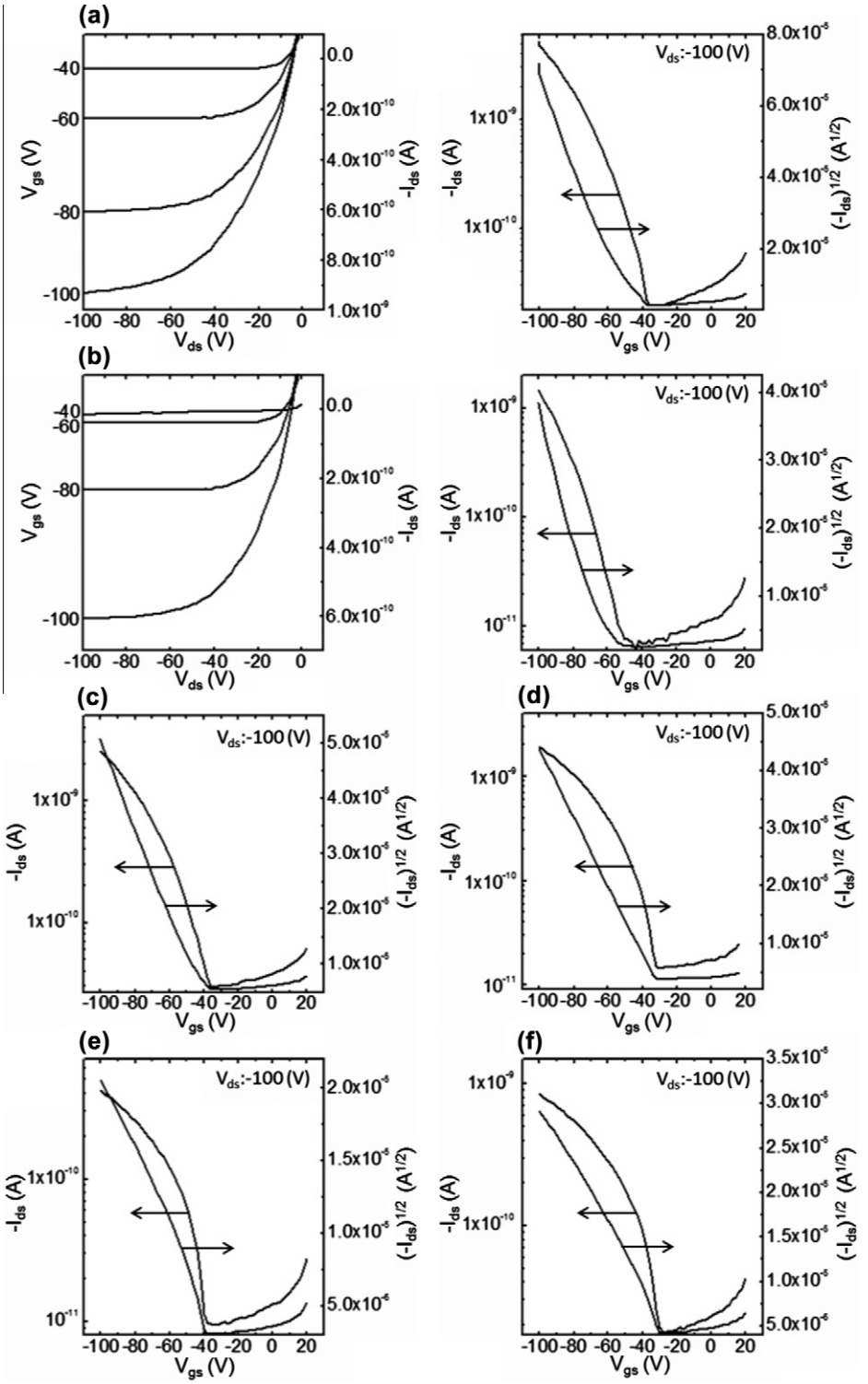

Fig. 3. Representative output (left) and transfer (right) curves for (a) immersion assembled and (b) spin coated BQT-PA SAMFET devices (L = 12 μm, W = 1000 μm). (c–f) Spin coated SAMFET transfer curves (L = 20, 30, 50, 80 μm, respectively, W = 1000 μm).

their monolayer. Regardless, due to the advantages conferred by phosphonic acid self assembly, SAMFET devices of this nature still need to be improved by further optimization of molecular design, processing, and device structure. In future studies, we plan to tailor molecular moieties of the π-conjugated segment, alkyl chain and

Table 1
Measured electrical characteristics of charge carrier mobility (μ), threshold voltage (V_t), and on/off current ratio (I_{on}/I_{off}) values with respect to SAMFET channel length. Immersion assembled (Imm), spun cast (SC), and bulk spun cast BQT-PA film (Bulk).

Channel length (μm)	μ ($\times 10^{-6}$ cm^2 V^{-1} s^{-1})	$-V_t$ (V)	I_{on}/I_{off}
12 (Bulk)	1.1–4.0	25–51	(1.0–3.3) $\times 10^2$
12 (Imm)	1.2–4.1	35–50	(2.0–5.4) $\times 10^2$
12 (SC)	1.3–8.0	32–53	(1.0–5.6) $\times 10^2$
20 (SC)	1.2–3.0	36–49	(1.0–2.1) $\times 10^2$
30 (SC)	1.7–2.1	30–48	(1.1–3.0) $\times 10^2$
50 (SC)	1.1–5.6	29–45	(1.5–2.2) $\times 10^2$
80 (SC)	1.1–4.0	31–42	(0.9–1.0) $\times 10^2$

Table 2
Comparison of high concentration (2 mM BQT-PA in chlorobenzene) immersion assembled devices and identical spun cast devices. Charge carrier mobility (μ) and number of functional 12 μm channel length devices in the set.

Immersion time	μ ($\times 10^{-6}$ cm^2 V^{-1} s^{-1})	Functional devices
Spun cast	1.2–4.2	8/10
1 min	None	0/10
5 min	None	0/10
10 min	0.02–0.1	4/10
30 min	0.5–1.1	7/10
1 h	1.4–3.8	8/10
5 h	1.1–4.0	9/10

binding group to optimize molecular orientation and packing for efficient intermolecular electronic wave function overlap and source/drain electrode–SAM contact. Despite low mobility, we do not observe significant variation between spin-coated and immersion assembly processed devices for channel lengths from 12 to 80 μm. Therefore, spin-coating of semiconducting phosphonic acid molecules may provide a viable processing route for rapid throughput of SAMFETs.

4. Conclusion

In conclusion, we have demonstrated a simple and generally applicable approach to fabricate SAMFETs through a rapid spin-coating process. Charge mobilities of 1.1–8.0 $\times 10^{-6}$ cm^2 V^{-1} s^{-1} were achieved for a wide range of channel lengths (from 12 to 80 μm). Characterization of the BQT-PA SAM was performed by AFM, ATR-FTIR, and NEXAFS, showing a densely packed monolayer with tilt angles of $\sim$32° and $\sim$44° for the thiophene rings and alkyl chains, respectively. This work is representative of major advancement in the processing of SAMFET devices, demonstrating that lengthy assembly procedures are not necessary to achieve high density SAMs capable of charge transport over long channel lengths.

Acknowledgements

This work is supported by the NSF-STC program under DMR-0120967, the AFOSR program under FA9550-09-1-0426. T. Weidner thanks the Deutsche Forschungsgemeinschaft for a research fellowship, and A.K.-Y. Jen thanks the World Class University (WCU) program through the National Research Foundation of Korea under the Ministry of Education, Science and Technology (R31-10035). Part of this work was conducted at the University of Washington NanoTech User Facility, a member of the NSF National Nanotechnology Infrastructure Network (NNIN).

References

[1] (a) J. Zaumseil, H. Sirringhaus, Chem. Rev. 107 (2007) 1296–1323;
(b) J.E. Anthony, Angew. Chem. Int. Ed. 47 (2008) 452–483;
(c) A.A. Virkar, S. Mannsfeld, Z.N. Bao, N. Stingelin, Adv. Mater. 22 (2010) 3857–3875;
(d) A.C. Arias, J.D. MacKenzie, I. McCulloch, J. Rivnay, A. Salleo, Chem. Rev. 110 (2010) 3–24;
(e) J. Sun, B. Zhang, H.E. Katz, Adv. Funct. Mater. 21 (2011) 29–45.
[2] C.R. Newman, C.D. Frisbie, D.A. da Silva Filho, J.-L. Brédas, P.C. Ewbank, K.R. Mann, Chem. Mater. 16 (2004) 4436–4451.
[3] H. Sirringhaus, Adv. Mater. 17 (2005) 2411–2425.
[4] Y. Cao, Z.M. Wei, S. Liu, L. Gan, X.F. Guo, W. Xu, M.L. Steigerwald, Z.F. Liu, D.B. Zhu, Angew. Chem. Int. Ed. 49 (2010) 6319–6323.
[5] G.S. Tulevski, Q. Miao, M. Fukuto, R. Abram, B. Ocko, R. Pindak, M.L. Steigerwald, C.R. Kagan, C. Nuckolls, J. Am. Chem. Soc. 126 (2004) 15048–15050.
[6] M. Mottaghi, P. Lang, F. Rodriguez, A. Rumyantseva, A. Yassar, G. Horowitz, S. Lenfant, D. Tondelier, D. Vuillaume, Adv. Funct. Mater. 17 (2007) 597–604.
[7] M. Novak, A. Ebel, T. Meyer-Friedrichsen, A. Jedaa, B.F. Vieweg, G. Yang, K. Voitchovsky, F. Stellacci, E. Spiecker, A. Hirsch, M. Halik, Nano Lett. 11 (2011) 156–159.
[8] E.C.P. Smits, S.G.J. Mathijssen, P.A. van Hal, S. Setayesh, T.C.T. Geuns, K.A.H.A. Mutsaers, E. Cantatore, H.J. Wondergem, O. Werzer, R. Resel, M. Kemerink, S. Kirchmeyer, A.M. Muzafarov, S.A. Ponomarenko, B. de Boer, P.W.M. Blom, D.M. de Leeuw, Nature 455 (2008) 956–959.
[9] V. Coropceanu, J. Cornil, D.A. da Silva Filho, Y. Olivier, R. Silbey, J.-L. Brédas, Chem. Rev. 107 (2007) 926–952.
[10] A.-M. Andringa, M.-J. Spijkman, E.C.P. Smits, S.G.J. Mathijssen, P.A. Hal, S. Setayesh, N.P. Willard, O.V. Borshchev, S.A. Ponomarenko, P.W.M. Blom, D.M. de Leeuw, Org. Electron. 11 (2010) 895–898.
[11] J. Randon, P. Blanc, R. Paterson, J. Membr. Sci. 98 (1995) 119–129.
[12] G. Guerrero, P.H. Mutin, A. Vioux, Chem. Mater. 13 (2001) 4367–4373.
[13] D.A. Outka, J. Stohr, J.P. Rabe, J.D. Swalen, J. Chem. Phys. 88 (1988) 4076–4087.
[14] K. Weiss, P.S. Bagus, C. Woll, J. Chem. Phys. 111 (1999) 6834–6845.
[15] O.M. Cabarcos, A. Shaporenko, T. Weidner, S. Uppili, L.S. Dake, M. Zharnikov, D.L. Allara, J. Phys. Chem. C 112 (2008) 10842–10854.
[16] N. Ballav, B. Schüpbach, O. Dethloff, P. Feulner, A. Terfort, M. Zharnikov, J. Am. Chem. Soc. 129 (2007) 15416–15417.
[17] J. Stöhr, NEXAFS Spectroscopy, vol. 25, Springer-Verlag, Berlin, 1992.
[18] O. Acton, D. Hutchins, L. Arnadottir, T. Weidner, N. Cernetic, G.G. Ting, T.-W. Kim, D.G. Castner, H. Ma, A.K.-Y. Jen, Adv. Mater. 23 (2011) 1899–1902.